ChemComm

COMMUNICATION

View Article Online
View Journal | View Issue

Cite this: *Chem. Commun.*, 2016, 52, 14458

Received 25th October 2016,
Accepted 24th November 2016

DOI: 10.1039/c6cc08586e

www.rsc.org/chemcomm

A photoswitchable rotaxane operating in monolayers on solid support†

Felix B. Schwarz,[a] Thomas Heinrich,[ab] Andreas Lippitz,[b] Wolfgang E. S. Unger*[b] and Christoph A. Schalley*[a]

A novel photoswitchable rotaxane was synthesised and its switching behaviour in solution was analysed with NMR and UV-Vis. A monolayer of rotaxanes was deposited on glass surfaces and the on-surface photoswitching was investigated. Angle-resolved NEXAFS spectra revealed a preferential orientation that reversibly changes upon switching.

Photochromic molecules are widely used as key components in stimuli-responsive molecular switches and machines. Common photoswitches like azobenzenes, spiropyranes and dithienylethenes offering a fast and clean photoisomerisation have been utilised in the development of complex functional systems and materials.[1–7] Especially, mechanically interlocked molecules (MIMs) like rotaxanes have been investigated intensely in this context.[1,5–7] The transfer of MIMs from solution into ordered arrays at interfaces is of great interest, as such order is the prerequisite for macroscopic effects through the concerted action of microscopic units.[8–11] Several examples for the deposition of MIMs on surfaces are reported in the literature.[12–14] However, there are only a few examples for surface-bound photoresponsive MIM-based systems.[15–17]

Recently, we reported the photoinduced pseudorotaxane formation of a photoresponsive axle and a tetralactam macrocycle carried out in solution and on surfaces with immobilized multilayers of macrocycles.[18] Here, we report a photoswitchable rotaxane, consisting of a tetralactam macrocycle (TLM) and a photoswitchable axle. The axle is comprised of an azobenzene photoswitch and a diketopiperazine binding site, which are both attached to a rigid xanthene backbone in a way that the azobenzene photoisomerisation influences the binding strength of the adjacent site by steric hindrance. By substitution with a suitable linker, this photoswitchable axle was used as the central building block for rotaxanes, serving as the photoswitch, the first binding site and the stopper simultaneously. The second part of the axle contains a diamide binding site,[19] which bears a bulky trityl stopper on one end and a linker unit at the other end. Rotaxanes **Rot1** and **Rot2** were obtained in a one-step ether-rotaxane synthesis from two axle building blocks and TLM **1** or **2** (Fig. 1). **Rot3** functionalised with a terpyridine unit at the TLM was synthesised in one step starting from **Rot2** in a Sonogashira coupling reaction with acetylene-functionalised terpyridine **3** (ESI†). **Rot1** containing the di-*tert*-butyl substituted TLM **1** was used for all solution studies due to its good solubility, while **Rot3** was used for surface experiments.

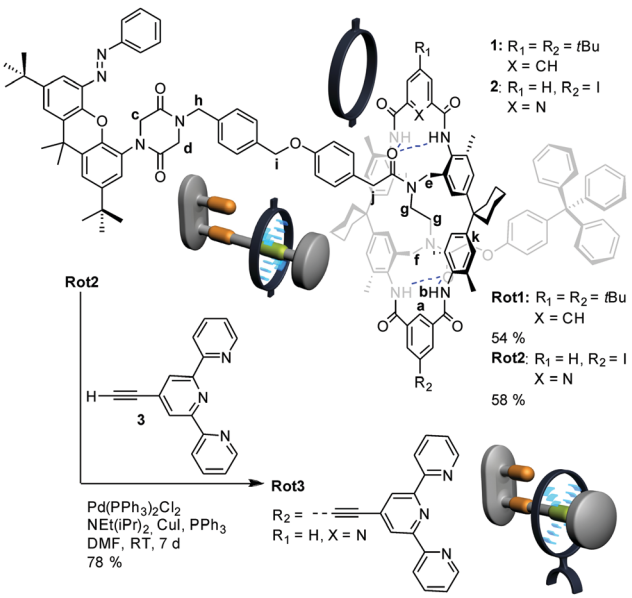

Fig. 1 Synthesis of photoswitchable rotaxanes **Rot1**, **Rot2** and **Rot3**.

The formation of **Rot1** was followed by ^{1}H NMR spectroscopy, confirming the threaded structure with the TLM being located at the diamide and not at the diketopiperazine binding site (Fig. 2d(i and ii) and ESI†). The mechanically interlocked

[a] *Institut für Chemie und Biochemie, Freie Universität Berlin, Takustr. 3, 14195 Berlin, Germany. E-mail: c.schalley@fu-berlin.de*

[b] *BAM – Federal Institute for Materials Research and Testing, Unter den Eichen 44-46, 12203 Berlin, Germany. E-mail: wolfgang.unger@bam.de*

† Electronic supplementary information (ESI) available: Experimental procedures, surface preparation, additional NMR, MS, XPS and NEXAFS data. See DOI: 10.1039/c6cc08586e

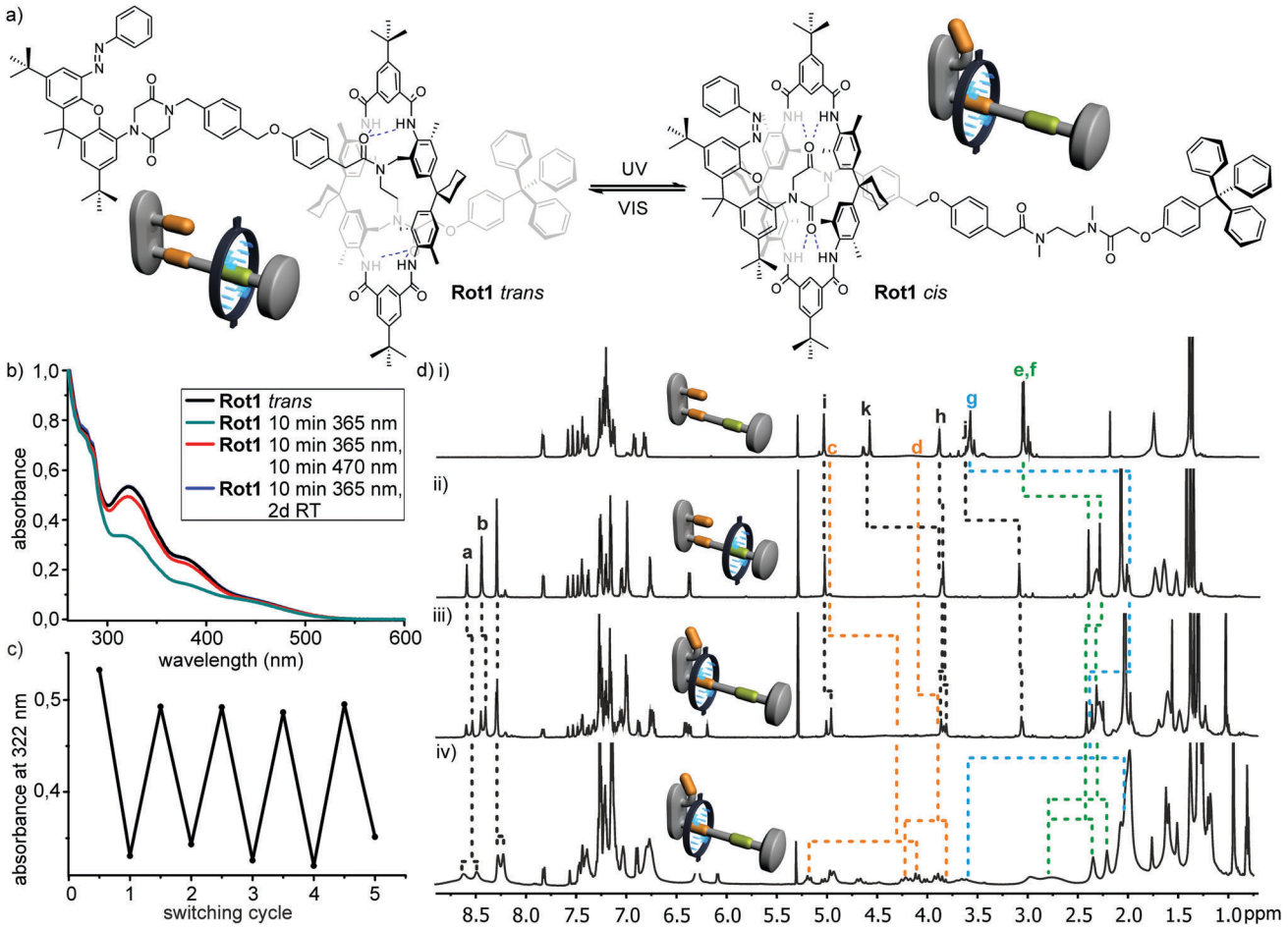

Fig. 2 (a) Photoswitching of **Rot1**. (b) UV-Vis spectra of *trans*-**Rot1** in CH_2Cl_2 (black), **Rot1** after 10 min irradiation at λ_1 = 365 nm (green), **Rot1** after irradiation at λ_1 = 365 nm and λ_2 = 470 nm for 10 min each (red), and **Rot1** after 10 min irradiation with 365 nm and subsequent equilibration for 2 d at 30 °C in the dark (blue, overlapping with black spectrum). (c) Reversibility of photoswitching of **Rot1** in CH_2Cl_2 tested by alternating irradiation at λ_1 = 365 nm and λ_2 = 470 nm for 10 min in each step. (d) ^{1}H NMR spectra of the free axle in $CDCl_3$ at RT (i), *trans*-**Rot1** in $CDCl_3$ at RT (ii), *cis* : *trans* 2 : 1 at RT (iii) and *cis* : *trans* 2 : 1 at 228 K (iv).

structure of **Rot1** was confirmed by IRMPD ESI-FTICR-MS experiments (ESI†).

The photoswitching of **Rot1** was studied in solution by UV-Vis and NMR spectroscopy. Photoisomerisation of the azobenzene group in **Rot1** from *trans* to *cis* was carried out by irradiation with an LED lamp at a wavelength of λ_1 = 365 nm. Back-switching was carried out by irradiation at λ_2 = 470 nm or thermal equilibration. The UV-Vis spectrum of *trans*-**Rot1** in CH_2Cl_2 displays a broad absorption band at *ca.* 520 nm and a characteristic absorption band for the $\pi \rightarrow \pi^*$ transition of azobenzene at 322 nm (Fig. 2b).[20] Irradiation at λ_1 = 365 nm leads to a decrease in intensity of the $\pi \rightarrow \pi^*$ absorption band, indicating the formation of *cis*-**Rot1**. Irradiating the sample at λ_2 = 470 nm induces back-switching to *trans*-**Rot1** up to *ca.* 90%. In both cases, the photostationary state was reached after 10 minutes. Complete back-isomerisation to *trans*-**Rot1** was accomplished by equilibrating the sample in the dark at 35 °C over two days. Reversibility was investigated by alternating irradiation at λ_1 = 365 nm and λ_2 = 470 nm over five cycles (Fig. 2c). ^{1}H NMR spectra of **Rot1** were measured before and after irradiation at λ_1 = 365 nm for 10 min (Fig. 2d(ii and iii)). In the spectrum after irradiation, a second set of signals for *cis*-**Rot1** is observed with a ratio of *cis*- : *trans*-**Rot1** of *ca.* 2 : 1. The protons a and b of the macrocycle undergo a small shift upfield in *cis*-**Rot1** compared to *trans*-**Rot1**, indicating a different binding situation. The protons c and d of the diketopiperazine site are shifted upfield by 0.73 and 0.15 ppm, while the protons e, f and g of the diamide site are shifted downfield by 0.05, 0.06 and 0.42 ppm. This leads to the conclusion that the macrocycle is moving from the diamide towards the diketopiperazine binding site. In comparison with the ^{1}H NMR spectrum of the free axle and the shifts observed in a previous binding study with the corresponding pseudorotaxane,[18] the shifts of the binding site protons c–g upon switching of **Rot1** are smaller than expected. Likely, the macrocycle undergoes a shuttling motion between the two binding sites which is fast on the NMR time scale (see below).

The binding constants for both binding sites in **Rot1** were determined by NMR titrations using structurally analogous model compounds containing one binding site each. For the diketopiperazine site, binding constants of 1650 ± 170 M^{-1}

when the azobenzene is in its *cis* configuration and $<15\ M^{-1}$ when the azobenzene is in the *trans* configuration were obtained.[18] For the diamide site, a binding constant of $1400 \pm 140\ M^{-1}$ was determined (ESI†). Although the diketopiperazine represents the favoured binding site, the small difference in binding energy will rather lead to a molecular shuttle than to a rotaxane switch with two distinct positions of the macrocycle.

Temperature-dependent NMR spectra in a range between 300 K and 228 K have been recorded to investigate the shuttling of *cis*-**Rot1** (ESI†). Upon cooling the sample, the peak for the macrocycle protons a at 8.52 ppm in the ^{1}H NMR spectra gets broadened, undergoes coalescence at approximately 243 K and splits into two signals at 8.63 and 8.50 ppm upon further cooling, indicating a shuttling motion which is slow on the ^{1}H NMR timescale. At 228 K, the signals for protons c and d of the diketopiperazine site split into two sets at 5.20 and 4.12 ppm for c respectively 4.24 and 3.87 ppm for d. The signals for the protons e, f, and g for the diamide site split as well into signals at 2.93 and 2.86 ppm for e, 2.25 and 2.86 ppm for f and 2.11 and 3.59 ppm for g (Fig. 2d(iv)). This implies that three different species are present: *trans*-**Rot1** with the macrocycle being located at the diamide site, *cis*-**Rot1** with the macrocycle being located at the diketopiperazine site and *cis*-**Rot1** with the macrocycle at the diamide site. Integration of the signals in the NMR spectrum at 228 K yields an overall ratio of **Rot1** with the macrocycle at the diketopiperazine site to **Rot1** with the macrocycle at the diamide site of approximately 2 : 3. Due to the very complex spectra and broad signals, a more detailed analysis of the shuttling behavior was not straightforward.

After the rotaxane switching was investigated in solution, the concept was transferred to surfaces by following previously established procedures for surface deposition.[21] A monolayer of rotaxanes was deposited on surfaces using metal–ion/pyridine/terpyridine coordination chemistry.[22–27] Cleaned glass slides have been used as the substrates for UV surface experiments and contact angle measurements, while silicon substrates were used for XPS and NEXAFS experiments. A self-assembled monolayer of **PDS** was deposited on the surface by immersing the substrate in a 5 mM solution of **PDS**. The surfaces were then treated with a 1 mM solution of tetrakis(acetonitrile)palladium(II) tetrafluoroborate to coordinate the pyridyl endgroups of **PDS** with palladium(II) ions, followed by immersion in a 1 mM solution of **Rot3** to create a monolayer of rotaxanes on the surface (Fig. 3a). The deposition of **Rot3** was followed by UV-Vis spectroscopy (Fig. 3b). As the glass slides absorb light below 300 nm, only the region above this value could be used. A substantial increase in absorbance was detected after deposition of **Rot3**, which resembles the UV-Vis spectra of **Rot1** in solution and therefore indicates a successful monolayer formation. XPS measurements show a molecular ratio of **Rot3** to **PDS** of 1 : 15.

To investigate on-surface switching, a surface functionalised with a monolayer of **Rot3** was irradiated with an LED lamp at a wavelength of λ_1 = 365 nm or λ_2 = 470 nm from a distance of about 20 cm. Different irradiation times were investigated and it was found that in case of λ_1 = 365 nm, no further changes in the absorbance spectra occurred after an irradiation time

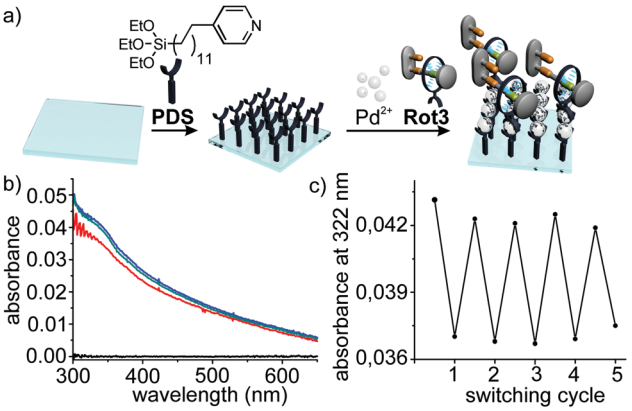

Fig. 3 (a) Surface deposition of **Rot3**, (b) transmission UV-Vis spectra of surfaces, **PDS** (black), **PDS**-Pd-**Rot3** (blue), **PDS**-Pd-**Rot3** 1 h 365 nm (red) and **PDS**-Pd-**Rot3** 1 h 365 nm, 1.5 h 470 nm (green; superimposing the blue curve), (c) reversibility of the on-surface photoswitching tested over five cycles.

of 1 h, while it took 1.5 h in case of λ_2 = 470 nm. After irradiation at λ_1 = 365 nm, the UV-Vis spectra of the surface showed a decrease in absorbance in the region between 300 and 500 nm, indicating the formation of *cis*-**Rot3**. After irradiation at λ_2 = 470 nm, the absorbance of the surface increased up to about 90% of its initial value, indicating almost complete back-switching to *trans*-**Rot3**. Reversibility was tested over five switching cycles (Fig. 3c). In a second approach, surfaces were functionalised with a covalently bound monolayer of rotaxanes by azide–alkyne click chemistry, which resulted in a similar photoswitchability, but a less dense packing (ESI†).

Contact angle measurements were conducted for a monolayer of **Rot3** that reveal a strong and reversible change in polarity upon photoswitching of the surfaces (ESI†). To prove successful rotaxane deposition and the structural effects of the rotaxane switching as well, angle-resolved C K-edge NEXAFS spectroscopy was conducted for the pristine rotaxane monolayer of **Rot3** on silicon, the monolayer after 1 h irradiation with λ_1 = 365 nm, and after 1 h light irradiation with λ_1 = 365 nm with subsequent 1.5 h irradiation at λ_2 = 470 nm as seen in Fig. 4. In the 55° C–K edge spectrum of the pristine rotaxane layer, the characteristic π* resonance splitting for pyridines and benzene is visible.[27] Furthermore, the peak at 285.4 eV is significantly more intense than the peak at 284.9 eV. Together with the intense π* resonance in the N–K edge spectrum (Fig. S28, ESI†) at 399.4 eV, which is characteristic for Pd-coordinated pyridine,[28] with a shoulder at 398.6 eV ($\pi^*_{O=C-N}$) characteristic for the axle molecule,[18] and with XPS data (Fig. S30 and S31, ESI†) this clearly indicates the successful deposition of the rotaxane. The pristine monolayer of *trans*-**Rot3** shows a relatively small, but clearly visible linear dichroism for the C K-edge π* and σ* resonances.[29] Irradiation with light at λ_1 = 365 nm results in a decrease of the linear dichroism in the C K-edge which is regained upon subsequent irradiation with λ_2 = 470 nm. In context of the solution study and the fact that the position of the macrocycle is fixed in *trans*-**Rot3**, but variable in *cis*-**Rot3**, a higher order in the monolayer when the rotaxane is switched to its *trans*-state can be assumed. The relatively small magnitude of

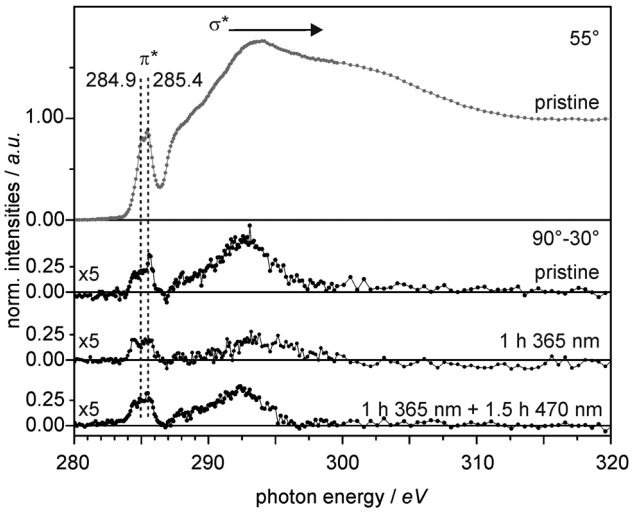

Fig. 4 55° C K-edge NEXAFS spectrum of the pristine rotaxane monolayer and its 90°–30° difference spectrum. Difference spectra after 1 h irradiation with λ = 365 nm, and after 1 h irradiation with λ = 365 nm followed by 1.5 h irradiation with λ = 470 nm (peak assignments are given in eV).

the linear dichroism effect might be due to a rather sparse packing in the monolayer resulting in lower preferential orientation of the immobilized molecules. Due to the exclusively photo-induced modification of the rotaxane states, the observed differences in linear dichroism can be associated with the switching states of **Rot3**. However, the analysis does not provide a quantification of the on-surface switching process.

In the present study, we developed a photoswitchable rotaxane and analysed its switching behavior in solution as well as in a monolayer of rotaxanes deposited on glass and silicon surfaces. NEXAFS spectroscopy revealed a preferential orientation in the monolayer, which reversibly changes upon photo switching of the rotaxane. In combination with chemically switchable rotaxanes, we are aiming for multi-stimuli responsive surface systems capable of performing concerted switching of distinct layers resulting in potential macroscopic effects.

We are grateful to the Deutsche Forschungsgemeinschaft (SFB 765) for funding. F. B. S. thanks the Beilstein Institut for a PhD fellowship. The authors thank Dr A. Nefedov (Karlsruhe Institute of Technology, KIT) from the HE-SGM Collaborate Research Group at the synchrotron facility BESSY II and Dr A. Vollmer and M. Mast (all HZB/BESSY II) for support during our activities at HZB. We thank Prof. Biprajit Sarkar for providing the catalyst for surface reactions.

Notes and references

1 N. Katsonis, M. Lubomska, M. M. Pollard, B. L. Feringa and P. Rudolf, *Prog. Surf. Sci.*, 2007, **82**, 407–434.
2 W. R. Browne and B. L. Feringa, *Annu. Rev. Phys. Chem.*, 2009, **60**, 407–428.
3 M.-M. Russew and S. Hecht, *Adv. Mater.*, 2010, **22**, 3348–3360.
4 R. Klajn, *Pure Appl. Chem.*, 2010, **82**, 2247.
5 M. Baroncini, G. Ragazzon, S. Silvi, M. Venturi and A. Credi, *Pure Appl. Chem.*, 2015, **87**, 537.
6 R. H. El Halabieh, O. Mermut and C. J. Barrett, *Pure Appl. Chem.*, 2004, **76**, 1445.
7 S. Erbas-Cakmak, D. A. Leigh, C. T. McTernan and A. L. Nussbaumer, *Chem. Rev.*, 2015, **115**, 10081–10206.
8 A. Coskun, M. Banaszak, R. D. Astumian, J. F. Stoddart and B. A. Grzybowski, *Chem. Soc. Rev.*, 2012, **41**, 19–30.
9 M. M. Boyle, R. A. Smaldone, A. C. Whalley, M. W. Ambrogio, Y. Y. Botros and J. F. Stoddart, *Chem. Sci.*, 2011, **2**, 204–210.
10 J. J. Davis, G. A. Orlowski, H. Rahman and P. D. Beer, *Chem. Commun.*, 2010, **46**, 54–63.
11 A. C. Fahrenbach, S. C. Warren, J. T. Incorvati, A.-J. Avestro, J. C. Barnes, J. F. Stoddart and B. A. Grzybowski, *Adv. Mater.*, 2013, **25**, 331–348.
12 V. Balzani, A. Credi and M. Venturi, *ChemPhysChem*, 2008, **9**, 202–220.
13 E. Coronado, P. Gavina and S. Tatay, *Chem. Soc. Rev.*, 2009, **38**, 1674–1689.
14 Y. Liu, A. H. Flood, P. A. Bonvallet, S. A. Vignon, B. H. Northrop, H.-R. Tseng, J. O. Jeppesen, T. J. Huang, B. Brough, M. Baller, S. Magonov, S. D. Solares, W. A. Goddard, C.-M. Ho and J. F. Stoddart, *J. Am. Chem. Soc.*, 2005, **127**, 9745–9759.
15 I. Willner, V. Pardo-Yissar, E. Katz and K. T. Ranjit, *J. Electroanal. Chem.*, 2001, **497**, 172–177.
16 P. Wan, Y. Jiang, Y. Wang, Z. Wang and X. Zhang, *Chem. Commun.*, 2008, 5710–5712.
17 J. Berna, D. A. Leigh, M. Lubomska, S. M. Mendoza, E. M. Perez, P. Rudolf, G. Teobaldi and F. Zerbetto, *Nat. Mater.*, 2005, **4**, 704–710.
18 F. B. Schwarz, T. Heinrich, J. O. Kaufmann, A. Lippitz, R. Puttreddy, K. Rissanen, W. E. S. Unger and C. A. Schalley, *Chem. – Eur. J.*, 2016, **22**, 14383–14389.
19 L. Kaufmann, E. V. Dzyuba, F. Malberg, N. L. Low, M. Groschke, B. Brusilowskij, J. Huuskonen, K. Rissanen, B. Kirchner and C. A. Schalley, *Org. Biomol. Chem.*, 2012, **10**, 5954–5964.
20 J. Griffiths, *Chem. Soc. Rev.*, 1972, **1**, 481–493.
21 C. H. H. Traulsen, V. Kunz, T. Heinrich, S. Richter, M. Holzweber, A. Schulz, L. K. S. von Krbek, U. T. J. Scheuschner, J. Poppenberg, W. E. S. Unger and C. A. Schalley, *Langmuir*, 2013, **29**, 14284–14292.
22 J. J. Richardson, M. Björnmalm and F. Caruso, *Science*, 2015, **348**, 6233.
23 V. Piñón and M. Weck, *Langmuir*, 2012, **28**, 3279–3284.
24 Y. Chaikin, H. Leader, R. Popovitz-Biro, A. Vaskevich and I. Rubinstein, *Langmuir*, 2011, **27**, 1298–1307.
25 P. C. Mondal, J. Yekkoni Lakshmanan, H. Hamoudi, M. Zharnikov and T. Gupta, *J. Phys. Chem. C*, 2011, **115**, 16398–16404.
26 G. de Ruiter, M. Lahav and M. E. van der Boom, *Acc. Chem. Res.*, 2014, **47**, 3407–3416.
27 N. Tuccitto, I. Delfanti, V. Torrisi, F. Scandola, C. Chiorboli, V. Stepanenko, F. Wurthner and A. Licciardello, *Phys. Chem. Chem. Phys.*, 2009, **11**, 4033–4038.
28 S. Richter, J. Poppenberg, C. H. H. Traulsen, E. Darlatt, A. Sokolowski, D. Sattler, W. E. S. Unger and C. A. Schalley, *J. Am. Chem. Soc.*, 2012, **134**, 16289–16297.
29 T. Heinrich, C. H. H. Traulsen, M. Holzweber, S. Richter, V. Kunz, S. K. Kastner, S. O. Krabbenborg, J. Huskens, W. E. S. Unger and C. A. Schalley, *J. Am. Chem. Soc.*, 2015, **137**, 4382–4390.